Journal of Applied Sciences

ISSN 1812-5654

science alert

ANSInet
an open access publisher
http://ansinet.com

Journal of Applied Sciences 10 (24): 3229-3235, 2010
ISSN 1812-5654
© 2010 Asian Network for Scientific Information

This article was presented in International Conference on Process Engineering and Advanced Materials 24th Symposium of Malaysian Chemical Engineers (15th-17th June, 2010)

Modeling and Simulation of Fixed Bed Adsorption Column using Integrated CFD Approach

S.A. Nouh, K.K. Lau and A.M. Shariff
Department of Chemical Engineering, Universiti Teknologi PETRONAS 31750, Tronoh, Malaysia

Abstract: The understanding of detailed fluid flow in the fixed bed adsorption column is substantially crucial since the mass and heat transfer in the bed is influenced by the column hydrodynamics. In this study, an integrated CFD model was developed to model and simulate the adsorption dynamics and hydrodynamics of gaseous fluid (CH_4 and CO_2 mixture) in the fixed bed adsorption column. The developed integrated model was used to determine the CO_2 concentration factor at the column (which indicating the CO_2 adsorption capacity) as a function of time, based on different operating conditions. The simulated results were compared with experimental data and found to give a good agreement with error less than 2.5%. The effect of various influencing parameters such as feed velocity, bed porosity and feed concentration were studied to investigate their influences on the CO_2 adsorption capacity. Besides, the effect of inlet CO_2 concentration on the bed temperature profile was also studied in the present study.

Key words: Computational fluid dynamics, fixed-bed adsorption, LDF model, 13X zeolite

INTRODUCTION

Generally, high CO_2 content in the Natural Gas (NG) potentially leads to many disadvantages including reduction in NG heating value and contribution to pipeline corrosion problems. Since most NG contains 70-90% of CH_4 and 0-20% of CO_2. Thus CH_4 was considered as only component representing NG and CO_2 as only impurity in this study. Various separation techniques are applicable for the removal of carbon dioxide, including adsorption, absorption and membrane separation. Pressure Swing Adsorption (PSA) system has been identified as one of the potential system for efficient removal of CO_2 from natural gas especially in producing high purity natural gas.

Several studies have been carried out to determine the most suitable adsorbent for the removal of CO_2 from its mixtures using the PSA system. Cavenati *et al.* (2004, 2006) have used 13X zeolite to selectively remove CO_2 from $CH_4/CO_2/N_2$ mixture. The 13X zeolite was found to be suitable for CO_2 separation, due to higher adsorption capacity of CO_2 on 13X zeolite which is much higher than for the other gases and on testing of several adsorbent. Similar results and conclusions were made by Gomes and Yee (2002).

To avoid the high cost of the experimental set-up for industrial scale-up, much interests and attentions have been devoted to the modeling of kinetic and equilibrium adsorption phenomena in the fixed bed adsorption column. Several popular mass transfer models are available in the literature for adsorption beds, such as pore-diffusion model, Linear Driving Force (LDF), etc. Details of these models were elaborated by Ruthven (1984), Yang (1987) and Ruthven *et al.* (1994). Simplified models are often obtained by using appropriate approximation in order to get substantial saving in computation time. Due to that, LDF model has been used by several researchers to predicate the kinetics of the CO_2 adsorption inside fixed bed column. Dong *et al.* (1999) conducted the separation of ternary gas mixture consisting of CO_2-CH_4-N_2, with three different adsorbents, activated carbon and 13 X zeolite and Carbon Molecular Sieve (CMS). The mass transfer between the two phases was simulated using LDF model under set of model assumption including negligible pressure drop, axial and radial dispersions. Besides Gomes and Yee (2002) has investigated the feasibility of CO_2 removal using PSA. A numerical simulation was carried out using Linear Driving Force (LDF) model to describe the adsorption kinetic. A good agreement was shown in the model prediction as well as a great purity of nitrogen gas recovered.

Recently, there has been intense interest in linking engineering models with rigorous simulation tools, parallel with the significant improvement in computational resources and codes. Simulation approaches potentially provides an attractive alternative to costly and time-consuming experimentation.

Computational Fluid Dynamics (CFD) simulation is appropriate to be used when the process performance is dictated by the fluid dynamics. CFD has been proposed as a reliable tool to model and simulate hydrodynamic, mass and heat transfer phenomena for the design and

Corresponding Author: K.K. Lau, Department of Chemical Engineering, Universiti Teknologi PETRONAS 31750, Tronoh, Malaysia

optimization of process equipment (Natarajan *et al*., 2005; Coussirat *et al*., 2007). Numerous CFD studies have been reported on the fluid flow and heat transfer in the packed bed reactors elsewhere (Baleo *et al*., 2000; Nijemeisland and Dixon, 2001; Coussirat *et al*., 2007; Guardo *et al*., 2007). Nevertheless, the CFD studies related to fixed bed adsorption have been found to be limited. Hence, there is a potential applicability of CFD to model transport phenomena and adsorption mechanism in packed bed CO_2 adsorption column. The aim of present study is to model and simulate the hydrodynamics and adsorption phenomena for the CO_2-CH_4 mixture in the fixed bed adsorption column filled with zeolite 13X. The effects of several important operating parameters were varied to study the influence of these parameters toward CO_2 adsorption efficiency. In this study, the adsorption isotherms of pure CO_2 and CH_4 on 13X zeolite were measured at constant temperature using gravimetric apparatus at maximum pressure of 6 bar. Full set of equilibrium data was fitted with the LDF model for the integrated CFD modeling.

MATERIALS AND METHODS

Experimental set-up for adsorption kinetic data: Adsorption equilibrium and kinetic of pure gases was performed in a (Rubotherm) gravimetric adsorption unit consists of two major components, which are Magnetic Suspension Balances (MSB) unit and the gas-dosing unit. A set-up of the equipment is shown in Fig. 1. The gas-dosing unit governs the amount and pressure of the gas in the system while the adsorption isotherm and kinetics are obtained from the magnetic suspension balance unit. The pressure of the system depends on the outlet pressure of the gas cylinder only without additional compressor. The temperature of the system is controlled by an electrical jacket heater and internal heat exchanger. The Magnetic Suspension Balance (MSB) is a very sensitive balance that is able to weigh samples contactless with a balance located at ambient conditions. The adsorbent sample is located in the measuring cell and can be coupled or decoupled from the balance by a contactless magnetic suspension coupling. The pressure of the system is governed by pressure transducer (PIRC) and dynamic valve for pressure range at 20-150 bar and another from 1-20 bar to acquire data at low and high pressures, respectively.

The 13X zeolite were supplied by Zeochem, Switzerland. Some of characteristic parameters of the adsorbent are summarized in Table 1, together with the experimental data of carbon dioxide adsorption equilibrium at 298 K.

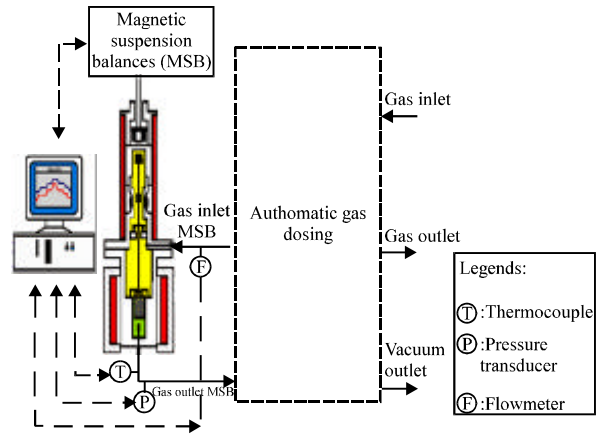

Fig. 1: Rubotherm MSB gravimetric adsorption measurement unit

Experimental set-up for model validation: The adsorption dynamic studies for model validation were carried out using two-bed Gas Adsorption Column Unit (GACU) developed in-house. The adsorption beds were made of stainless steel with a length of 0.3 and 0.038 m Internal Diameter (ID) and wall thickness of 0.007 m. The beds were packed with 13X zeolite particles. The column designed for pressure up to 20 bar and temperature up to 923 K. Two pressure transducers were located at the feed and bed ends in order to measure bed pressure variation, in this study the pressure drop of the column was very small (<0.1 bar) and cannot detected accurately with the pressure transducer. The feed flow was controlled by a mass flow controller (Brook, 5851i±0.05 NL min^{-1}). In order to keep the pressure in the adsorption bed constant, manual backpressure regulator (Swaglelok 4R3A) was installed with RIX micro boost compressor. The concentration variations of the effluents at the adsorption and desorption steps were analyzed by Gas Chromatography (GC) analysis system. Sampling in the GC was carried out automatically via a Gas Sampling Valve (GSV) at specific time (2 min). The feed gases for the adsorption process were nitrogen (as inert gas), carbon dioxide and methane supplied from gas cylinder. All gas used has purity more than 99.9% and were supplied by MOX Sdn. Bhd. The details of the operating conditions are shown in Table 1.

Mathematical model: The dynamics behavior of the fixed-bed adsorption column can be modeled and characterized using the integrated CFD model. In order to formulate a generalized model corresponding to the adsorption mechanism, following assumptions were made:

- The heat transfer within the bed is neglected
- Competitive adsorption between CO_2 and CH_4 was assumed
- The Linear Driving Force (LDF) model was used for representing the mass transfer into the pellets
- The mass transfer coefficient is lumped of the external fluid film resistance and marcropore diffusion
- The porosity was uniform and constant
- Instantaneous equilibrium between the bulk and pellet concentrations

Governing equations for adsorption column

Continuity equation: The general 3-D continuity equation for unsteady-state fluid flow is:

$$\frac{\partial \rho}{\partial t}+\frac{\partial \rho u}{\partial x}+\frac{\partial \rho v}{\partial y}+\frac{\partial \rho w}{\partial z}=0 \tag{1}$$

Navier-stokes equations

To represent the fluid flow through the porous medium, additional sources term, S_{ix}, S_{iy}, S_{iz} were added to Eq. 2-4 to model the flow resistance in 3D dimensions as follows:

Navier-stokes equation in x-direction

$$\begin{aligned}&\frac{\partial(\rho u)}{\partial t}+\frac{\partial(\rho uu)}{\partial x}+\frac{\partial(\rho vu)}{\partial y}+\frac{\partial(\rho wu)}{\partial z}=-\frac{\partial P}{\partial x}+2\frac{\partial}{\partial x}(\mu\frac{\partial u}{\partial x})\\&-\frac{2}{3}\frac{\partial}{\partial x}[\mu(\frac{\partial u}{\partial x}+\frac{\partial v}{\partial y}+\frac{\partial w}{\partial z})]+\frac{\partial}{\partial y}[\mu(\frac{\partial u}{\partial y}+\frac{\partial v}{\partial x})]+\frac{\partial}{\partial z}[\mu(\frac{\partial u}{\partial z}+\frac{\partial w}{\partial x})]+S_{ix}\end{aligned} \tag{2}$$

Navier-stokes equation in y-direction

$$\begin{aligned}&\frac{\partial(\rho v)}{\partial t}+\frac{\partial(\rho vv)}{\partial y}+\frac{\partial(\rho uv)}{\partial x}+\frac{\partial(\rho wv)}{\partial z}=-\frac{\partial P}{\partial y}+2\frac{\partial}{\partial y}(\mu\frac{\partial v}{\partial y})\\&-\frac{2}{3}\frac{\partial}{\partial y}[\mu(\frac{\partial u}{\partial x}+\frac{\partial v}{\partial y}+\frac{\partial w}{\partial z})]+\frac{\partial}{\partial x}[\mu(\frac{\partial v}{\partial x}+\frac{\partial u}{\partial y})]+\frac{\partial}{\partial z}[\mu(\frac{\partial v}{\partial z}+\frac{\partial w}{\partial y})]+S_{iy}\end{aligned} \tag{3}$$

Navier-Stokes Equation in z-direction

$$\begin{aligned}&\frac{\partial(\rho w)}{\partial t}+\frac{\partial(\rho ww)}{\partial z}+\frac{\partial(\rho uw)}{\partial x}+\frac{\partial(\rho vw)}{\partial y}=-\frac{\partial P}{\partial z}+2\frac{\partial}{\partial z}(\mu\frac{\partial w}{\partial z})\\&-\frac{2}{3}\frac{\partial}{\partial z}[\mu(\frac{\partial u}{\partial x}+\frac{\partial v}{\partial y}+\frac{\partial w}{\partial z})]+\frac{\partial}{\partial x}[\mu(\frac{\partial w}{\partial x}+\frac{\partial u}{\partial z})]+\frac{\partial}{\partial y}[\mu(\frac{\partial w}{\partial y}+\frac{\partial v}{\partial z})]+S_{iz}\end{aligned} \tag{4}$$

The porous medium momentum source term S_i calculates the pressure gradient in the packed bed and creates a pressure drop that is proportional to the fluid velocity (or velocity squared) as shown below:

$$S_i=\frac{\mu}{\alpha}u_i+C_2(\frac{1}{2}\rho u_i|u_i|) \tag{5}$$

Where:

$$C_2=\frac{1.75}{D_P}\frac{(1-\varepsilon)}{\varepsilon^3} \tag{6}$$

$$\alpha=\frac{D_P^2}{150}\frac{\varepsilon^3}{(1-\varepsilon)^2} \tag{7}$$

where, C_2 and α, are the inertia resistance and viscous resistant coefficient, which estimated using Eq. 6 and 7.

Gases mass balance equation: The mass balance for the bulk flow in the fixed bed column is given by Eq. 8:

$$-D_{z,i}\frac{\partial^2 C_i}{\partial x_i^2}+\frac{\partial u_i C}{\partial x_i}+\frac{\partial C_i}{\partial t}+[\frac{1-\varepsilon}{\varepsilon}]\frac{\partial q_i}{\partial t}=0 \tag{8}$$

The adsorption rate $\partial q_i/\partial t$ was obtained based on the LDF model (Yang, 1987) as shown:

$$\rho_s\frac{\partial q_i}{\partial t}=k_i a(C_i-C_i^p) \tag{9}$$

where, C_i is the bulk concentration (kg m^{-3}), C_i^p is the pellet concentration (kg m^{-3}), t is the time (s), ϵ is the bed voidage fraction, $D_{z,i}$ is the column 3-D dispersion coefficient, k_i is the average mass transfer coefficient for each species and a the surface area of pellet per volume of bed.

The column dispersion coefficient, $D_{z,i}$ in Eq. 8 can evaluated by Ruthven (1984):

$$D_{z,i}=0.7\,D_m+vRp \tag{10}$$

The molecular diffusivity, D_m can be calculated by Suzuki (1989):

$$D_m=1.8583\times10^{-3}\times\frac{T^{\frac{3}{2}}(\frac{1}{M_A}+\frac{1}{M_B})^{\frac{1}{2}}}{P\sigma_{AB}^2\Omega_{AB}} \tag{11}$$

where, A = CO_2 and B = CH_4

The concentration inside a spherical pellet C_i^p is described by multi-component Langmuir model (Suzuki, 1989).

$$q_i=\frac{q_s K_A C_A}{1+K_A C_A+K_B C_B} \tag{12}$$

As shown in Eq. 12, q_i is the average adsorbed concentration (kg m^{-3}), q_s is the adsorbent maximum capacity concentration. Equation 8, 9 and 12 are coupled

in order to solve the overall column mass balance by calculating the concentration within the pellet C_i^p with considering the interaction between the two components by using the multi-component Langmuir model.

Vant Hoff correlation was used to estimate the equilibrium constant K_A (Suzuki 1989).

$$K_A = K_0 \exp(-\Delta H_A/RT) \quad (13)$$

where, R is the ideal gas law constant, T is the operation temperature, $K_0 = 0.0206$ is the pre-exponential factor and $\Delta H_A = -15.294$ kJ mol^{-1} is the heat of CO_2 adsorption.

Besides, the mass transfer coefficient (k_A) for CO_2 is given by Yang (1987):

$$k_A = \frac{D_m}{2R_p}(1.09/\varepsilon)Sc^{0.33}Re^{0.33} \quad (14)$$

where, Sc, Re and R_p are the Schmidt numbers, Reynolds numbers and the pellet radius, respectively.

Energy balance equation: The overall energy balance for the bulk flow in the fixed bed column including the heat generated by adsorption was given by Yang (1987):

$$\rho_g C_{pg}\frac{\partial T}{\partial t} - K_L\frac{\partial^2 T}{\partial z^2} + \varepsilon\rho_g C_{pg}(u\frac{\partial T}{\partial z}) = -\rho_B(\Delta\overline{H_i})x\sum_{i=1}^{n}\frac{\partial q_i}{\partial t} \quad (15)$$

where, K_L is the mixture axial thermal conductivity (W/m.K), ρ_g is the mixture density, C_{pg} is the heat capacity and $\ddot{A}H_i$ is the heat of adsorption (kJ mol^{-1}).

BOUNDARY CONDITION AND COMPUTATIONAL METHOD

One of the important sections of CFD modeling is the construction of the mesh geometry topology. The mesh establishes the accuracy of the simulation. It has to be chosen with enough detail to describe the processes accurately and with a degree of coarseness that enables solution within an acceptable amount of time. This study focused mainly on maintaining a 3D topology that described the physical model accurately and has been able to handle the flow specifics of the fixed bed column geometry.

Considering a three-dimensional axisymmetric domain, the above set of model Eq. 1-15 were solved using commercial software FLUENT 6.3 (FLUENT, 2003). The generalized balances that used by the FLUENT 6.3 were the governing equations for conservation of mass and momentum, which coupled with system mass balance equation. The basic equations and background of these balances are stated in the FLUENT 6.3 User's Guide (FLUENT, 2003). In order to simulate the transport equations and adsorption phenomena in the fixed bed adsorption column using FLUENT 6.3 software, extra scalars would be needed. User-defined scalars (UDS) have been used to implement the flow mass transfer coefficients, which were modeled using user-define source terms. To determine the interaction between the mass and heat balances for the adsorption system (which is an exothermal process), vant Hoff correlation (Eq. 13) have been used to represent the interaction between the amounts of mass adsorbed and the temperature elevation. C programming language has been used to write the codes in the User's Defined Functions (UDF) file for customizing the UDS equations.

Table 1: Experimental data and simulation boundary conditions

Adsorbent properties	
Type	Zeolite13X (sphere)
Porosity	0.72 dimensionless
Bulk density	650 kg m^{-3}
Equilibrium data for CO_2 adsorption (obtained from MSB)	
Pressure (P)	1-60 bar
Temperature (T)	298 K
Maximum capacity (q_s)	5.7 mmol g^{-1}
Equilibrium constant (K_i)	2.37
Adsorption columns (for gas adsorption unit)	
Inside diameter	0.038 m
Outside diameter	0.045 m
Wall thickness	0.007 m
Bed length	0.5 m
Bed porosity	0.4 dimensionless
Bed weight	0.25 kg
Simulation boundary conditions (for model validation)	
Pressure	10 bar
Inlet velocity	0.044 m sec^{-1}
Temperature	298 K
CO_2 inlet concentration	0.8939 kg m^{-3}
CH_4 inlet concentration	0.33395 kg m^{-3}

Table 1 summarizes the experimental parameters and simulation boundary conditions for the CFD model validation.

RESULTS AND DISCUSSION

CFD model validation: The integrated CFD model was used (as described in section II) to determine the CO_2 concentration factor at the column outlet for different time based on different operating conditions. The results simulated using the CFD model, were compared with the experimental data as shown in Fig. 2. Based on the results, the simulated data demonstrated a good agreement with the experimental data with maximum error less than 2.5%.

Based on the good agreement of the model results, several important operating parameters were varied to study the influence of these parameters on CO_2 adsorption performance.

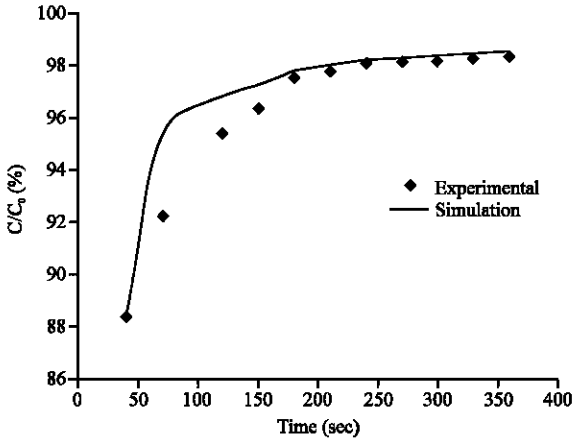

Fig. 2: Comparison of CO_2 experimental and simulation breakthrough curve (Sampled at column outlet)

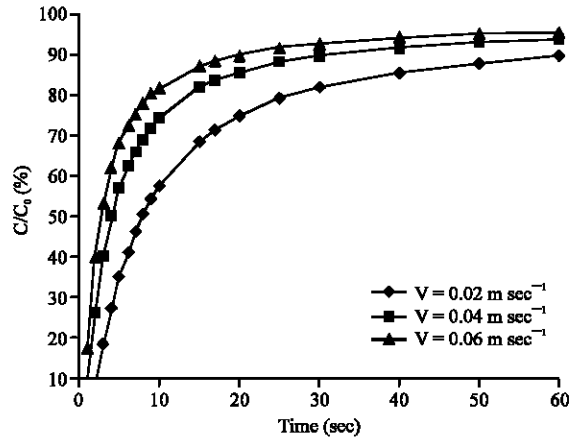

Fig. 3: Effect of feed velocity on the simulated breakthrough curve (Sampled at column outlet)

Effect of feed velocity: Figure 3 shows the effect of feed velocity for CO_2 adsorption process in the fixed bed adsorption column. The CO_2 concentration, C, was sampled at the column outlet. The effect of feed velocity was studied at 0.02, 0.04 and 0.06 m sec^{-1}, while the CO_2 inlet concentration, C_0 in each run was kept constant at 50% of CO_2 concentration. Based on the figure, as the velocity increases, the breakthrough curve becomes steeper. This signifies that higher CO_2 concentration is produced in the product stream, under higher feed velocity. At higher velocity, the gas mixture would have shorter residence time in the fixed bed column. Under this condition the gas mixture would leave the column before the equilibrium adsorption of CO_2 occurs. Thus, higher feed velocity tends to give a reduction in removal efficiency of CO_2 in the fixed bed adsorption column.

Effect of bed porosity: Figure 4 shows the effect of bed porosity on the breakthrough curve. The CO_2

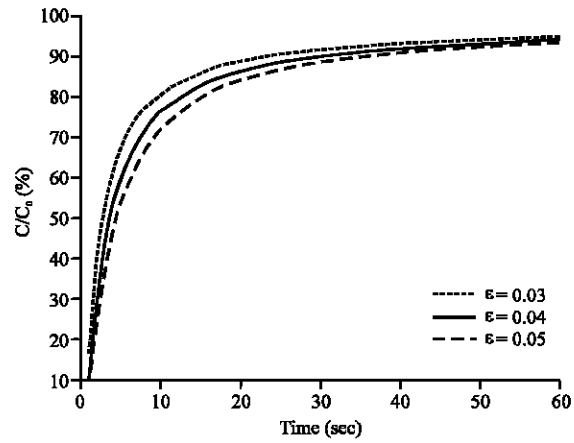

Fig. 4: Effect of bed porosity on the simulated breakthrough curve (Sampled at column outlet)

concentration, C, was sampled at the column outlet. Based on the figure, as the bed porosity increases from 0.3 to 0.5, higher CO_2 concentration is produced at the product stream. This signifies that the increment of bed porosity leads to a lower performance in CO_2 removal, which gives higher CO_2 concentration at the column outlet. This trend can be explained by the effect of the fluid flow through a packed-bed. Since the closeness and orientation of the packing has significant effect on the pressure gradient and velocity magnitude, smaller bed porosity leads to an increase in the bed velocity and consequently reduces the gas residence time in the bed.

This would give a higher CO_2 concentration at the product stream. Nevertheless, based on the mass balance Eq. 8 and 9, the porosity has an inverted effect, whereas, smaller bed porosity tends to increase the adsorption rate and reduce the CO_2 concentration at the outlet. Hence, based on Fig. 4, it can be concluded that the influence of hydrodynamics is more dominant as compared to the effect of mass transfer for the adsorption of CO_2 in the fixed bed column.

Effect of CO_2 concentration on the adsorption process: Figure 5 shows the effect of CO_2 concentration factor (C/C_0) inside the fixed bed adsorption column at different adsorption time (5, 30 and 120 sec). Three different CO_2 concentrations (10, 30 and 70%) were varied to study the adsorption capacity, which can be calculated based on column CO_2 concentration factor (C/C_0), where higher concentration factor represents lower adsorption capacity. Under the case with 10% of CO_2 feed concentration, a rapid increasing of CO_2 concentration factor was observed in the adsorption column (from 5 to 30 sec). As the adsorption process proceeds to 120 sec, the fixed bed adsorption process tends to give a uniform

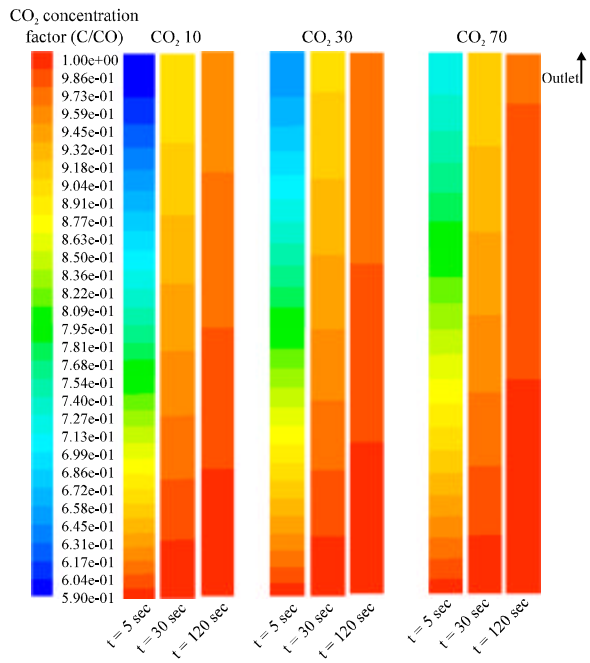

Fig. 5: Effect of CO_2 concentration on the simulated adsorption process

CO_2 concentration factor throughout the entire column. The rapid increasing of bed concentration at the beginning of the adsorption time (5 to 30 sec) was due to the high affinity of the fresh adsorbent to adsorbe, which derived from the physical Van der Waals and electrostatic Forces (Slejko, 1985). When the adsorption approaches to the equilibrium, the adsorbent capacity reduces as the bed becomes saturated.

Comparing with other cases with different CO_2 feed concentration, higher CO_2 feed concentration (70%) tends to give a higher CO_2 concentration factor (lower adsorbent capacity) for the entire column bed under each of the adsorption time studied. This results exhibit that higher CO_2 feed concentration tends to achieve bed saturation and equilibrium at a shorter period of time.

Effect of CO_2 concentration on the temperature profile: Figure 6 shows the evolution of temperature profile at different CO_2 concentrations (10, 30 and 50%). The temperature profile was sampled at the column outlet. Since CO_2 adsorption is an exothermic process, the column temperature tends to increase with CO_2 concentration. This is exhibited in Fig. 6, where the column initial temperature (283 k) was found to increase during the range of adsorption period from 283 to 296 K, 309 and 317 K at 10, 30 and 50% of CO_2 concentration respectively. This phenomenon is due to the proportional

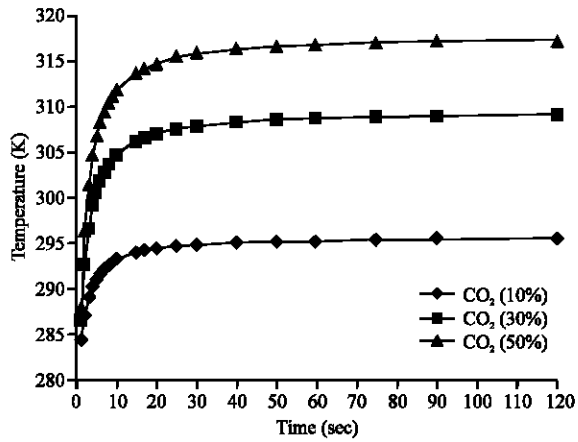

Fig. 6: Effect of CO_2 concentration on the simulated temperature profile (Sampled at column outlet)

relation between the adsorbed amount and the temperature releases. The gradient of the temperature increment is found to be higher at the beginning of the adsorption (<30 sec), where the adsorption rate of the CO_2 is higher at each given concentration. When the adsorption time approaches 60s, the temperature gradient achieves developed stage, where further increment is relatively small compared with the adsorption time. This is due to the saturation of CO_2 in the adsorbent bed.

CONCLUSION

Integrated CFD model was employed to simulate the transport and adsorption phenomena of the CO_2-NG fixed bed adsorption column. The hydrodynamics and mass transfer models were validated with experimental data. Under present study, several important operating parameters were studied and the results showed a reasonable manner for the effect of feed velocity, bed porosity and CO_2 inlet concentration. This study also showed that the hydrodynamics within the packed beds significantly influences the performance and capability of the adsorption process.

NOTATIONS

a	:	Surface area of pellet per volume of bed
C_0	:	Inlet concentration (kg m^{-3})
C	:	Bed concentration (kg m^{-3})
C_2	:	Inertia resistance coefficient (m)
D_m	:	Molecular diffusivity (m^2 sec^{-1})
D_p	:	Particles diameter (m)
$D_{z,i}$	:	The column 3D dispersion coefficient (m)
K	:	Equilibrium constant
k	:	Mass transfer coefficient (sec^{-1})

$M_{A,B}$: Species molecular weight (g mol^{-1})
P : Partial pressure (Pa)
q : Adsorbent capacity (mmol g^{-1})
q_s : Maximum capacity (mmol g^{-1})
t : Time (sec)
u : Gas velocity (x-direction) (m sec^{-1})
v : Gas velocity (y-direction) (m sec^{-1})
w : Gas velocity (z-direction) (m sec^{-1})

Greek symbols

ϵ : Bed voidage fraction (Porosity)
ρ_s : Particles Density (kg m^{-3})
ρ : Fluid Density (kg m^{-3})
α : Viscous resistant coefficient (m^{-1})
μ : Fluid Viscosity (Ns m^{-2})
Ω_{AB} : Collision integral, a function of k_BT/ϵ_{AB} where k_B is Boltzmann's constant
σ_{AB} : Lennard-Jones constant

Abbreviation

CFD : Computational Fluid Dynamics
LDF : Linear Driving Force
UDS : User's Defined Scalars
UDF : User's Defined Functions
NG : Natural Gas

ACKNOWLEDGMENTS

The authors gratefully acknowledge the support from University Technology PETRONAS by providing grant and facilities for the research.

REFERENCES

Baleo, J.N., A. Subrenat and P. le Cloirec, 2000. Numerical simulation of flows in air treatment devices using activated carbon cloths filters. Chem. Eng. Sci., 55: 1807-1816.

Cavenati, S., C.A. Grande and A.E. Rodrigues, 2004. Adsorption equilibrium of methane, carbon dioxide and nitrogen on zeolite 13X at high pressure. J. Chem. Eng. Data, 49: 1095-1101.

Cavenati, S., C.A. Grande and A.E. Rodrigues, 2006. Separation of CH_4, CO_2 and N_2 mixtures by layer pressure swing adsorption for upgrade of natural gas. Chem. Eng. Sci., 60: 3893-3906.

Coussirat, M., A. Guardo, B. Mateos and E. Egusquiza, 2007. Performance of stress-transport models in the prediction of particle-to-fluid heat transfer in packed beds. Chem. Eng. Sci., 62: 6897-6907.

Dong, F., H. Lou, A. Kodama, M. Goto and T. Hirose, 1999. The petlyuk PSA process for the separation of ternary gas mixtures: Exemplification by separation a mixture of CO_2-CH_4-N_2. Separat. Purif. Technol., 16: 159-166.

FLUENT, 2003. FLUENT 6.3 Users Guide Manual. Fluent Inc., Lebanon, New Hampshire, USA.

Gomes, V.G. and K.W.K. Yee, 2002. Pressure swing adsorption for carbon dioxide sequestration from exhaust gases. Separat. Purif. Technol., 28: 161-171.

Guardo, A., M. Coussirat, F. Recasens, M.A. Larrayoz and X. Escaler, 2007. CFD studies on particle-to-fluid mass and heat transfer in packed beds: Free convection effects in supercritical fluids. Chem. Eng. Sci., 62: 5503-5511.

Natarajan, S., C. Zhang and C. Briens, 2005. Numerical simulation and experimental verification of gas flow through packed beds. Power Technol., 152: 31-40.

Nijemeisland, M. and A.G. Dixon, 2001. Comparison of CFD simulations to experiment for convective heat transfer in a gas–solid fixed bed. Chem. Eng. J., 82: 231-246.

Ruthven, D.M., 1984. Principles of Adsorption and Adsorption Processes. Wiley-Interscience, New York, pp: 433.

Ruthven, D.M., S. Farooq and K.S. Knaebel, 1994. Pressure Swing Adsorption. VCH Publishers, New York, Cambridge, pp: 352.

Slejko, F.L., 1985. Adsorption Technology: A Step Approach to Process Evaluation and Application. Marcel Dekker, New York.

Suzuki, M., 1989. Adsorption Engineering. Elsevier, New York.

Yang, R.T., 1987. Gas Separation by Adsorption Processes. Buterworth, New York.